

Assessing the seismic vulnerability of single-family residential buildings in the Khorezm region

Ravshan Savutov¹, Alisher Shamuratov², Vakhitkhan Ismailov³, Sharofiddin Yodgorov⁴, Akbarjon Abdunazarov⁵

^{1,2}Urgench State University, 14 Hamid Olimjon Street, Urgench 220100, Uzbekistan

^{3,4}Institute of Seismology of Academy of Sciences of Republic of Uzbekistan, Tashkent 100128, Uzbekistan

⁵Namangan State Technical University, House 12, I. Karimov Street, New Namangan District, Namangan City, 160100, Uzbekistan

⁴Corresponding author

E-mail: ¹rsavutov@mail.ru, ²ashamurotov1996@gmail.com, ³vakhit.mbm@gmail.com,

⁴sh.i.yodgorov@gmail.com, ⁵abdunazarovakbar16@gmail.com

Received 25 February 2026; accepted 23 April 2026; published online 8 June 2026

DOI <https://doi.org/10.21595/vp.2026.26187>



76th International Conference on Vibroengineering in Tashkent, Uzbekistan, April 28-29, 2026

Copyright © 2026 Ravshan Savutov, et al. This is an open access article distributed under the Creative Commons Attribution License, which permits unrestricted use, distribution, and reproduction in any medium, provided the original work is properly cited.

Abstract. The effect of seismic waves on detached rammed earth and adobe-brick buildings in the Khorezm region, along with an assessment of the buildings' vulnerability, was numerically modeled using the PLAXIS 3D software package, which is based on the finite element method. The maximum amplitudes of displacements, velocities, and accelerations were determined at pre-selected observation points on the building. A comparative analysis was conducted to examine the relationship between the effect of seismic waves and the building type. A model of a detached building in the Khorezm region was developed. Rammed earth and mud-brick were adopted as the building materials. The calculation results showed that the rammed earth building, having a higher mass, was at greater risk of brittle failure due to the generation of high inertial forces during an earthquake. In contrast, the mud-brick building is considered a relatively lightweight structure, and its safety level is increased by reinforcement with a seismic belt and connecting elements. In seismic zones and areas with high soil moisture, it is advisable to use lightweight structural systems.

Keywords: seismic zone, adobe building, unfired brick, seismic safety, building, seismic waves, finite element method, soil-structure interaction, PLAXIS 3D.

1. Introduction

Earthquakes are among the most dangerous natural phenomena, posing a serious threat to the safety of buildings and structures. Uzbekistan is located in a seismically active zone [1]-[4]. In seismically active regions, the stability and safety level of residential buildings are directly dependent on their structural system, construction materials, mass, rigidity, and soil conditions. In many regions of Uzbekistan, particularly in the Khorezm province, individually constructed low-rise residential buildings are primarily built from traditional construction materials – rammed earth and adobe bricks [5]. These materials are widely used due to their economic advantages and good thermal properties; however, their strength under seismic impact has not been sufficiently studied.

The seismic resistance of buildings with rammed earth and adobe bricks depends on numerous factors, among which the structure's mass, rigidity, the quality of inter-element connections, and the presence of seismic reinforcement elements play a crucial role [6]. Heavy, high-mass structures generate significant inertial forces during an earthquake, which increases the risk of brittle failure. In contrast, relatively lightweight structural systems can perform better under dynamic loading conditions if they are reinforced with seismic belts and connecting elements. Therefore, identifying and assessing the seismic vulnerability of traditional building systems is of

great scientific and practical importance.



Fig. 1. Current state of residential buildings in the Khorezm region, Uzbekistan. Photo by Ravshan Savutov in Shovot district, Madaniyat MFY, “Bunyodkor” street, on November 11, 2025

2. Methods

When solving this problem, the length of the selected model is 100 m, the width is 50 m, and the depth is 40 m. The 1st layer has a sandy soil depth of 2 m and the 2nd layer has a fine sand depth of 38 m, the groundwater level is located at a depth of 3 m, the building is 23.3 m long, 15 m wide, and 3.20 m high.



Fig. 2. Exterior view of the building. Photo by Ravshan Savutov in Shovot district, Katqal’a MFY, “Billur” street, on February 19, 2026

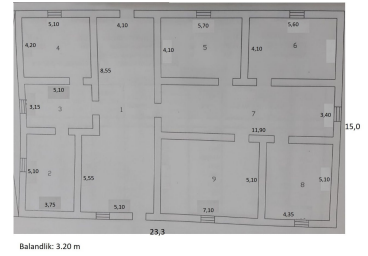


Fig. 3. Building wall plan

We consider the problem as one of wave propagation in an inhomogeneous half-space within the theory of elasticity. After placing a building on the boundary of the half-space, the problem becomes an inhomogeneous one with complex geometry, which cannot be solved using analytical methods. Therefore, we will solve the problem using numerical methods, specifically the finite element method. It is known that numerical methods cannot be applied to an infinite domain. Consequently, we replace the infinite half-space with a finite domain - a parallelepiped [7]. In this case, the following conditions, which ensure that the waves propagate towards infinity, are imposed on the boundaries; please refer to Eq. (1):

$$\begin{aligned}
 & \left. \begin{aligned} \sigma_x &= a\rho V_p \dot{u} \\ \tau_{xy} &= b\rho V_s \dot{v} \\ \tau_{xz} &= b\rho V_s \dot{w} \\ \sigma_y &= -a\rho V_p \dot{u} \end{aligned} \right\} \text{On ADHJ} & \left. \begin{aligned} \sigma_x &= -a\rho V_p \dot{u} \\ \tau_{xy} &= -b\rho V_s \dot{v} \\ \tau_{xz} &= -b\rho V_s \dot{w} \\ \sigma_z &= a\rho V_p \dot{w} \end{aligned} \right\} \text{On BCEF} & \left. \begin{aligned} \sigma_y &= a\rho V_p \dot{u} \\ \tau_{yz} &= b\rho V_s \dot{w} \\ \tau_{yx} &= b\rho V_s \dot{v} \end{aligned} \right\} \text{On ADCB} \\
 & \left. \begin{aligned} \tau_{yz} &= -b\rho V_s \dot{w} \\ \tau_{yx} &= -b\rho V_s \dot{v} \end{aligned} \right\} \text{On HJFE} & \left. \begin{aligned} \tau_{zy} &= b\rho V_s \dot{u} \\ \tau_{zx} &= b\rho V_s \dot{v} \end{aligned} \right\} \text{On AHBE}
 \end{aligned} \quad (1)$$

Free-field boundary conditions were assigned in the x -direction, while no special boundary condition was applied in the y -direction. A compliant base was used at the bottom boundary in the z -direction. These conditions were applied to the corresponding faces of the computational domain, namely ADHJ and BCEF, ADCB and HJFE, and AHBE, as illustrated in Fig. 4.

The study area was divided into 10 042 finite elements and 24 658 nodes. The finite elements were chosen to have the shape of irregular tetrahedra. The order of the system of differential equations of motion was $24\ 658 \times 3 = 73\ 974$ (Fig. 5). Properties of the soil are listed in Table 1.

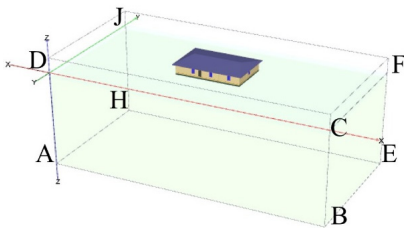


Fig. 4. Setting boundary conditions

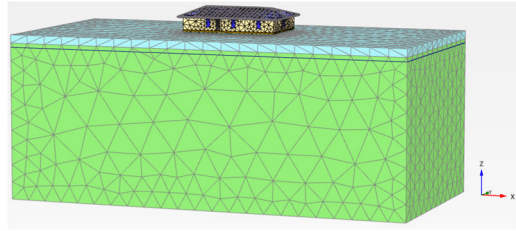


Fig. 5. Splitting the model into finite elements

Table 1. The characteristics of the building material and soil being modeled are given

Name	Unit of measurement	Designation	Name of the soil	
			Loam soil	Fine sand soil
General characteristics of the soil				
Soil model	–	–	Mohr-Coulomb	Mohr-Coulomb
Soil feature	–	–	Dried	Dried
The specific gravity of the upper layer of the soil under the influence of underground water	kN/m ³	γ_{unsat}	15.6	15.60
The specific gravity of the bottom layer of the soil under the influence of underground water	kN/m ³	γ_{sat}	18.6	19.70
Initial porosity coefficient	–	e_{init}	0.728	0.710
Young's modulus (constant)	kN/m ²	E	15000	35000
Poisson's ratio	–	ν	0.30	0.3
Longitudinal wave velocity	m/s	V_p	60.23	92.1
Shear wave velocity	m/s	V_s	112.7	172.1
Material properties			Rammed earth	Adobe brick
Model type	–	–	Elastic	Elastic
Modulus of elasticity	kN/m ²	E	180000	150000
Poisson coefficient	–	ν	0.3	0.25
Density	kN/m ³	ρ	18.5	18
Poisson ratio	–	%	5	5

The system of differential equations describing the motion of a mechanical system under a dynamic load is expressed as follows, please refer to Eq. (2):

$$[M]\{\ddot{u}(t)\} + [C]\{\dot{u}(t)\} + [K]\{u(t)\} = \{F(t)\}, \quad (2)$$

where, $[M]$ is the mass matrix, $[C]$ is the damping matrix, $[K]$ is the stiffness matrix, and $\{F\}$ is the dynamic load vector. The vectors $\{u\}$ – displacement, $\{\dot{u}\}$ – velocity, and $\{\ddot{u}\}$ – acceleration are continuous functions of time [8]-[9].

When an earthquake occurs, the propagating seismic waves affect the ground surface through a dynamic load. In this case, we assume that the wave propagates along the x -axis. Taking into account the physical and mechanical properties of the material, we determine the displacements, velocities, and accelerations at the nodes within the soil.

In the present study, seismic excitation was introduced using the recorded acceleration time history of a real earthquake event rather than an analytical wave expression. The prescribed input motion can be written as $\ddot{u}_g(t) = \text{arcc}(t)$, where $\text{arcc}(t)$ is the recorded ground acceleration as

a function of time. Therefore, the dynamic loading in the numerical model was applied through the real accelerogram shown in Fig. 6(a).

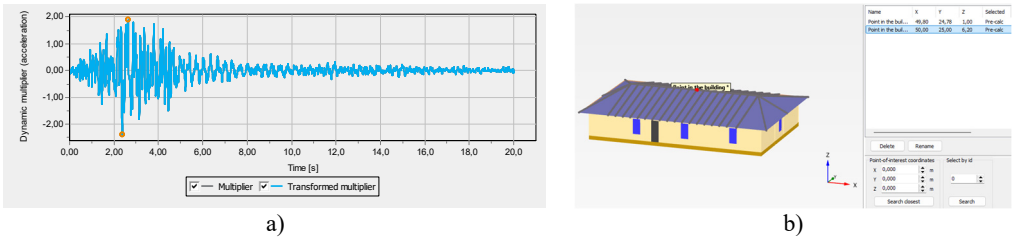


Fig. 6. a) The acceleration time history of the Kobe 1995 earthquake was used as dynamic input for the numerical analysis. The Kobe 1995 earthquake record was selected due to its well-documented characteristics and strong ground motion intensity. Its frequency content is comparable to seismic conditions observed in Central Asia; b) an observation point in the building

3. Results and discussion

To evaluate the effect of seismic waves on the building, the maximum values of displacement u_x , velocity v_x , and acceleration a_x at selected observation points were comparatively analyzed.

Fig. 7 shows the maximum displacement u_x along the x -axis at the floor level. The results indicate that the maximum displacement for the rammed earth building was $u_{xmax} = 239.65$, while for the adobe brick building it was $u_{xmax} = 239.64$ mm. The values are nearly identical, indicating that both structures have similar overall stiffness characteristics. This suggests that displacement alone is not sufficient to assess seismic performance differences between the two building types.

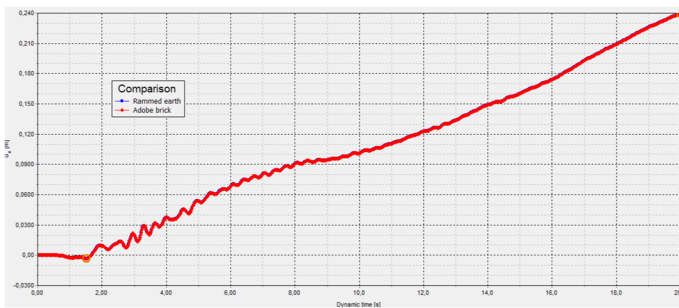


Fig. 7. Building floor displacement comparison chart

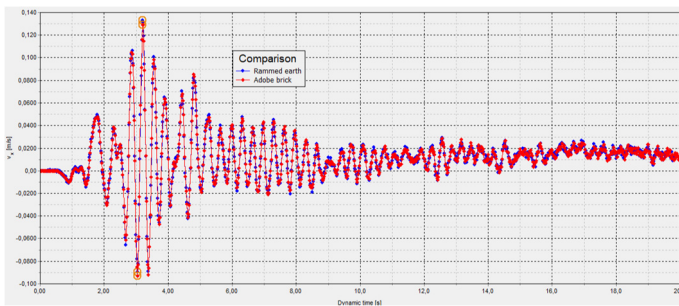


Fig. 8. Velocity comparison graph for the building's floor level

Fig. 8 presents the comparison of velocity v_x at the floor level. The maximum velocity for the rammed earth building was $v_{xmax} = 13.30$ cm/s, whereas for the adobe brick building it was $v_{xmax} = 12.91$ cm/s. This represents a reduction of approximately 3 % for the adobe structure. The lower velocity response can be attributed to the reduced mass and stiffness of the adobe material,

which leads to decreased dynamic energy transfer during seismic excitation.

Fig. 9 illustrates the acceleration a_x response at the same observation level. The maximum acceleration for the rammed earth building was $a_{xmax} = 228.25 \text{ cm/s}^2$, while for the adobe brick building it was $a_{xmax} = 211.51 \text{ cm/s}^2$, corresponding to a reduction of approximately 7.3 % in the adobe structure.

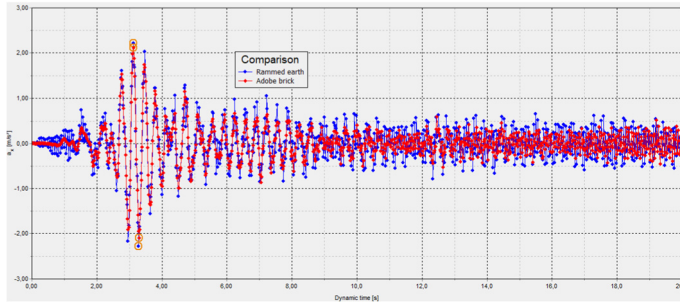


Fig. 9. Graph comparing acceleration at the building's floor level

Since acceleration is directly related to inertial forces, higher acceleration values result in increased seismic forces acting on the structure. In the case of the rammed earth building, its higher mass leads to greater inertial forces, making it more susceptible to brittle failure.

To further assess seismic vulnerability, the obtained acceleration values were interpreted in terms of potential structural damage. It is well established that structures made of brittle materials, such as rammed earth and adobe, possess low tensile strength and are highly sensitive to dynamic loading. Therefore, increased acceleration levels may lead to cracking, deformation, and eventual structural failure.

The results indicate that the higher acceleration observed in rammed earth buildings corresponds to a greater seismic vulnerability. In contrast, adobe brick structures, due to their lower mass and reduced inertial response, demonstrate relatively improved seismic performance under identical loading conditions.

Overall, the findings confirm that structural mass plays a key role in seismic response. Lighter adobe brick buildings exhibit better dynamic performance compared to heavier rammed earth structures under seismic excitation.

4. Conclusions

This study investigated the seismic response of single-family residential buildings constructed from rammed earth and adobe bricks in the Khorezm region using numerical modeling in PLAXIS 3D based on the finite element method, considering soil-structure interaction under seismic loading. The results demonstrate that although both building types exhibit nearly identical displacement values, significant differences are observed in velocity and acceleration responses. In particular, the maximum acceleration in rammed earth buildings reached 228.25 cm/s^2 , whereas in adobe brick buildings it was 211.51 cm/s^2 , corresponding to a reduction of approximately 7.3 %.

Since acceleration is directly related to inertial forces, these results indicate that rammed earth structures are subjected to higher dynamic forces, increasing their susceptibility to cracking and brittle failure. In contrast, adobe brick buildings, due to their lower mass and reduced inertial response, demonstrate improved seismic performance under identical loading conditions.

Therefore, seismic vulnerability is strongly governed by structural mass and material properties. Heavier structures tend to develop larger inertial forces, leading to increased damage potential, while lighter systems exhibit more favorable dynamic behavior.

From an engineering perspective, the findings suggest that the use of lightweight construction materials and proper structural reinforcement (such as seismic belts and connections) can

significantly enhance seismic safety in regions with similar soil and seismic conditions.

It should be noted that this study is limited by the use of a single earthquake record and simplified material assumptions. Future research should incorporate multiple seismic inputs and detailed damage modeling, including crack propagation and plastic strain distribution.

Overall, this study provides a quantitative basis for assessing seismic vulnerability of traditional residential buildings and contributes to the development of more effective seismic design strategies in earthquake-prone regions.

Acknowledgements

The authors have not disclosed any funding.

Data availability

The datasets generated during and/or analyzed during the current study are available from the corresponding author on reasonable request.

Conflict of interest

The authors declare that they have no conflict of interest.

References

- [1] V. A. Ismailov, S. I. Yodgorov, S. B. Allayev, T. U. Mamarozikov, and S. B. Avazov, "Seismic microzoning of the Tashkent territory based on calculation methods," *Soil Dynamics and Earthquake Engineering*, Vol. 152, p. 107045, Jan. 2022, <https://doi.org/10.1016/j.soildyn.2021.107045>
- [2] V. A. Ismailov, S. I. Yodgorov, A. S. Khusomiddinov, E. M. Yadigarov, B. U. Aktamov, and S. B. Avazov, "Regional seismic risk assessment based on ground conditions in Uzbekistan," *Natural Hazards and Earth System Sciences*, Vol. 24, No. 6, pp. 2133–2146, Jun. 2024, <https://doi.org/10.5194/nhess-24-2133-2024>
- [3] V. Ismailov, S. Yodgorov, B. Aktamov, S. Avazov, A. Azamjonov, and D. Jumaev, "Assessment of damage to residential buildings in a scenario-based strong earthquake in the fergana valley region," *Vibroengineering Procedia*, Vol. 60, pp. 91–96, Dec. 2025, <https://doi.org/10.21595/vp.2025.25309>
- [4] A. Kayumov, A. Khisomiddinov, O. Zafarov, I. Ruziyev, and K. Ergashev, "Effect of vibration on the calculated resistance of sandy soils," *Vibroengineering Procedia*, Vol. 60, pp. 68–74, Dec. 2025, <https://doi.org/10.21595/vp.2025.25554>
- [5] S. Takhirov, K. M. Mosalam, M. A. Moustafa, L. Myagkova, and B. Quigley, "Laser scanning, modeling, and analysis for damage assessment and restoration of historical structures," in *Proceedings of the 5th International Conference on Computational Methods in Structural Dynamics and Earthquake Engineering (COMPADYN 2015)*, pp. 2375–2395, Jan. 2015, <https://doi.org/10.7712/120115.3545.1384>
- [6] S. Takhirov, B. Rakhmonov, M. Akhmedov, and M. Blondet, "Structural health monitoring of Chadra Hauly (Khorezm, Uzbekistan) by means of laser scanning," in *AIP Conference Proceedings*, Vol. 3282, No. 1, p. 030017, Apr. 2025, <https://doi.org/10.1063/5.0266557>
- [7] S. Yuldashev, A. Abdunazarov, S. Jumaboyeva, M. Boytemirov, and Y. Tillaboyev, "Attenuation of seismic surface waves affecting the building using various barriers," in *AIP Conference Proceedings*, Vol. 3282, No. 1, p. 030016, Apr. 2025, <https://doi.org/10.1063/5.0265304>
- [8] Y. Jumatov and R. Savutov, "Justification of parameters and operating modes of a screw feed chopper for livestock farms," *IOP Conference Series: Earth and Environmental Science*, Vol. 1420, No. 1, p. 012022, Jan. 2024, <https://doi.org/10.1088/1755-1315/1420/1/012022>
- [9] A. Yuvmitov, D. Akhundjanov, U. Abdurakhmanov, N. Khasanova, and B. Egamberdiev, "Study of stress-strain state of structures and assessment of seismic safety of Ismoil Somoni Mausoleum in Bukhara," *E3S Web of Conferences*, Vol. 452, p. 06007, Nov. 2023, <https://doi.org/10.1051/e3sconf/202345206007>